Effect of grain boundary on the buckling of graphene nanoribbons

M. Neek-Amal and F. M. Peeters

Citation: Applied Physics Letters **100**, 101905 (2012); doi: 10.1063/1.3692573
View online: http://dx.doi.org/10.1063/1.3692573
View Table of Contents: http://scitation.aip.org/content/aip/journal/apl/100/10?ver=pdfcov
Published by the AIP Publishing

Effect of grain boundary on the buckling of graphene nanoribbons

M. Neek-Amal[1,a)] and F. M. Peeters[2]
[1]*Department of Physics, Shahid Rajaee Teacher Training University, Lavizan, Tehran 16785-136, Iran*
[2]*Departement Fysica, Universiteit Antwerpen, Groenenborgerlaan 171, B-2020 Antwerpen, Belgium*

(Received 15 June 2011; accepted 18 February 2012; published online 6 March 2012)

The buckling of graphene nano-ribbons containing a grain boundary is studied using atomistic simulations where free and supported boundary conditions are invoked. We consider the buckling transition of two kinds of grain boundaries with special symmetry. When graphene contains a large angle grain boundary with $\theta = 21.8°$, the buckling strains are larger than those of perfect graphene when the ribbons with free (supported) boundary condition are subjected to compressive tension parallel (perpendicular) to the grain boundary. This is opposite for the results of $\theta = 32.2°$. The shape of the deformations of the buckled graphene nanoribbons depends on the boundary conditions, the presence of the particular used grain boundaries, and the direction of applied in-plane compressive tension. © *2012 American Institute of Physics*. [http://dx.doi.org/10.1063/1.3692573]

Large area graphene sheets have been grown on metallic foils which were found to contain grain boundaries.[1] Scanning tunneling microscopy experiments were used to investigate tilt grain boundaries in graphite.[2] Transmission electron microscopy was able to observe individual dislocations in graphene.[3] The effect of grain boundaries on both electronic and mechanical properties of graphene was investigated theoretically by Yazyev and Louie.[4] Recently Huang *et al*. used transmission electron microscopy and found hundreds of grains and grain boundaries in a graphene sheet and revealed that they weaken the mechanical strength of the graphene membranes while they do not influence strongly their electrical properties.[5] Depending on the grain boundary structure, high transparency and perfect reflection of charge carriers over remarkably large energy ranges was reported by using first principle calculations.[6] The effects of grain boundaries on the buckling of nano-scale graphene nanoribbons (GNR) has not been investigated up to now, while it is important for their mechanical stability.

Recently, we studied the effect of applied external axial stress on the thermomechanical properties of perfect graphene (PG)[7,8] and GNRs containing randomly distributed vacancies.[9] In this paper, we address the effect of the presence of these grain boundaries with special symmetry (having angles $\theta = 21.8°$ and $\theta = 32.2°$) and in-plane boundary compressive stress applied in two different directions, on the buckling and the stability of GNR for the case of supported boundary (SBC) and free boundary conditions (FBCs). We found that the presence of the studied grain boundaries (1) alters the sine wave shape of the longitudinal deformation modes of GNR when subjected to SBC, (2) when subject to compressive tension perpendicular to the grain boundary with $\theta = 21.8°$, the GNR buckles at smaller (larger) strains as compared to perfect graphene in case of FBC (SBC), (3) the buckling transition found for compressive tension parallel to the grain boundary with $\theta = 21.8°$ is three times larger than the one for perfect graphene subjected to compressive tension along the zig-zag direction, (4) the buckling transition for graphene containing a grain boundary with $\theta = 32.2°$ is smaller than for $\theta = 21.8°$ and is independent of the used boundary conditions, and (5) free energy calculations reveal that a grain boundary with $\theta = 32.2°$ becomes unstable when subjected to compressive tension.

Initially the coordinates of all atoms are put in a flat surface of a honey-comb lattice with nearest neighbor distance equal to $a_0 = 0.142$nm. Our perfect GNR (PG) is a rectangular GNR with dimensions $a \times b = 20 \times 10$ nm^2 in x and y directions with armchair (ac) and zigzag (zz) edges, respectively. A grain boundary is introduced as an array of 5-7 defects, which are put in the center of the PG along the y-direction with angle θ (see Fig. 1). As an example, we study two kinds of grain boundaries which were named LAGBI and LAGBII by Yazyev and Louie.[4] These grain boundaries are typical interfaces between domains of graphene with different crystallographic orientation. Mutual orientations of the two crystalline domains are described by the misorientation angle which for LAGBI is $\theta = 21.8°$ and for LAGBII is $\theta = 32.2°$.

In Fig. 1, we depict two snap shots of the central portion of LAGBI (a) and LAGBII (b) after relaxation at room temperature.

Classical atomistic molecular dynamics simulations (MD) are employed to simulate compressed PG, LAGBI, and LAGBII using Brenner's bond-order potential[10] and temperature is controlled by a Nose-Hoover thermostat at room temperature. Before starting the compression, the systems are equilibrated during 75 ps (150 000 time steps). Extra atoms were added to the boundaries of the rectangular samples which are characterized by $x = \pm a/2 \pm 2$Å, $y = \pm b/2 \pm 2$Å. The compression and boundary conditions (FBC and SBC) are applied on these extra atoms which are outside the main systems.

Compressing direction is defined by the angle "α". For example, $\alpha = 0(\pi/2)$ implies that compression is applied in the x-direction (y-direction) so that the right (up) longitudinal ends at $x > a/2$ ($y > b/2$) are under compressive tension in $-x$ ($-y$)-direction and left longitudinal ends at $x < -a/2$ ($y < -b/2$) are under compressive tension in x (y)-direction

[a)]Author to whom correspondence should be addressed. Electronic mail: mehdi.neekamal@gmail.com.

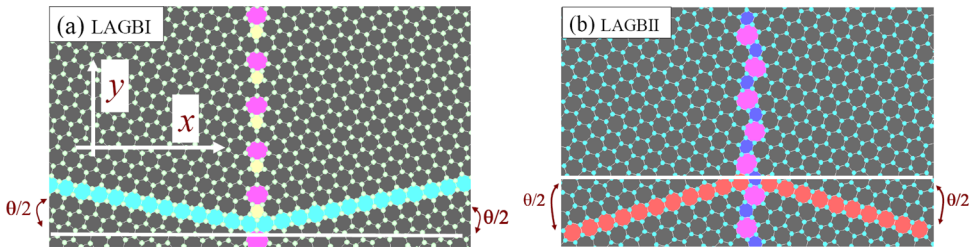

FIG. 1. (Color online) Two snap shots taken from the central portion of GNRs with grain boundaries after relaxation at room temperature. Two different configurations of the grain boundaries (LAGBI in (a) with $\theta = 21.8°$ and LAGBII in (b) with $\theta = 32.2°$, see Ref. 4) are shown by the colored pentagon and heptagons.

(see Fig. 1 in Ref. 7). Note that only in PG "ac"("zz") direction is equivalent to x-direction (y-direction). For the lateral ends (for $\alpha = 0$ they are $|y| > b/2$ and for $\alpha = \pi/2$ they are $|x| > a/2$), we used SBC (only movement of atoms in lateral ends in the compression direction is allowed not in the z-direction) and FBC. The FBC (SBC) condition is equivalent to suspended graphene at two longitudinal ends that is put over a trench while it is free at the lateral two ends.[11] Supported boundary condition can be created in experiments by suspending graphene from two longitudinal ends and supporting the other two lateral ends to a substrate which prevents graphene to move vertically.[12]

We applied a strain rate $\nu = 0.027$/ns and $\nu = 0.054$/ns for $\alpha = 0$ and $\alpha = \pi/2$, respectively. The strain rate is given by $\nu = 2\delta x/5000l\delta t$, where $\delta t = 0.5$ fs is our MD-simulation time step, $\delta x = 0.667$ pm is used as the compression step after each 5000 steps and the factor two is because the compression is applied on two longitudinal ends (for more details see Ref. 7). Here $l = a$ or $l = b$ if $\alpha = 0$ or $\alpha = \pi/2$, respectively. Notice that the atoms in the longitudinal ends are fixed during each compression step.

We use the Jarzynski equality,[13] i.e., $\Delta F = -\beta^{-1}\ln\langle\exp(-\beta W)\rangle$, which gives a relation between the difference of the free energy and the total work done on the system (W) during a non-equilibrium evolution where $\beta = 1/k_B T$. The averaging is done over several realizations of the paths between the initial and the final state. We found that averaging over 10 simulations with different initial states for each particular case results in a sufficient accurate value for ΔF (more technical details can be found in Refs. 8 and 14).

Elasticity theory predicts that the shape of the lowest mode of the buckled state (of a simple bar with length l, under axial symmetric load applied at its longitudinal ends and free from lateral ends) is half a sine wave, i.e., $\delta w = \tilde{w}\sin(\pi x/l)$, where δw is the transverse deflection.[7,15]

For a rectangular plate subjected to the SBC, elasticity theory[7,15] predicts the following possible deformations $\delta w = \sum_{m,n=1}^{\infty} \tilde{w}_{mn}\sin(n\pi x/a)\sin(m\pi y/b)$, where (m, n) are integers in order to satisfy the SBC and $\tilde{w}_{mn}$ is the amplitude of each mode (m, n). Including the appropriate strain energy and using δw, the minimum buckling boundary stress for the considered systems always occurs for $m = 1$ and various values of n. It is equivalent to a single half wave in the lateral direction and various harmonics n in the direction of compression (i.e., perpendicular to the grain boundary).

From our simulations, we found that after many compression steps GNRs starts to buckle, but the shape of the deformed GNRs was found to depend strongly on the presence of the grain boundary and on the direction of applied compression.

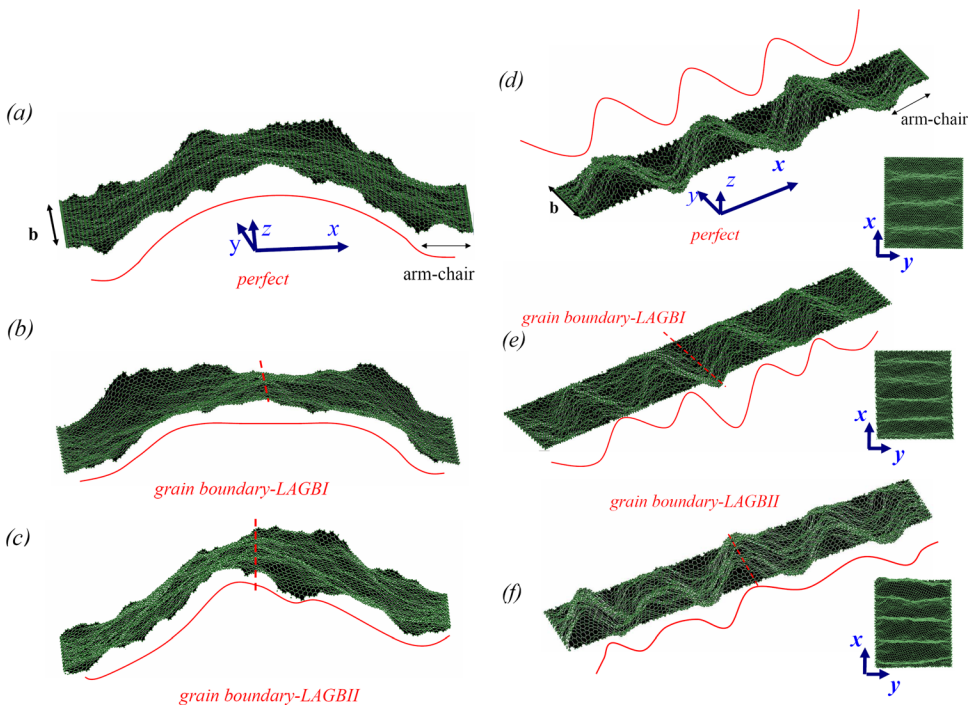

FIG. 2. (Color online) Snap shots of buckled graphene with free lateral boundary condition (a)–(c) and supported lateral boundary condition (d)–(f) for perfect graphene (a),(d), graphene with LAGBI type grain boundary (b),(e), and graphene with LAGBII type grain boundary (c),(f) where $\epsilon = 2.45\%$, $\alpha = 0$. The red curves give the z-deviation averaged over the y-direction (to improve visualization the z-components of all atoms were scaled by a factor of 3 and the edge atoms were excluded). The insets show top views of each right hand side panel.

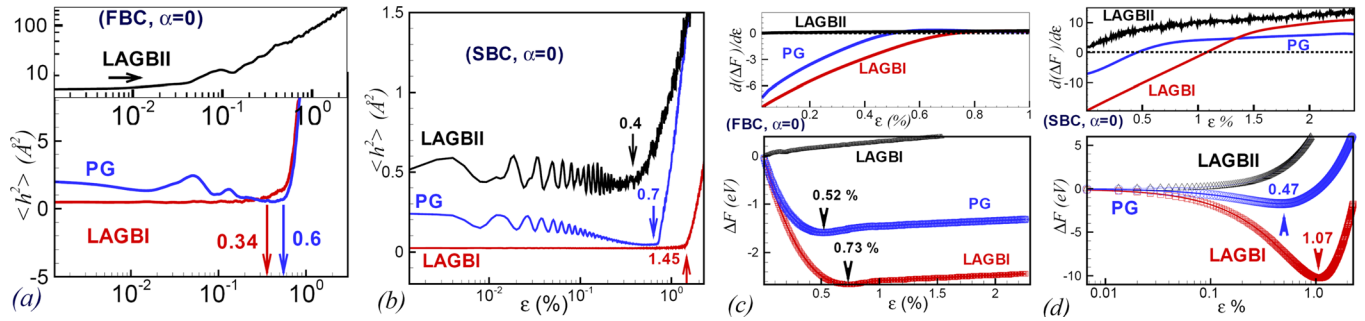

FIG. 3. (Color online) (a) The out of plane displacement versus applied strain for graphene with free lateral boundary condition (a) and supported lateral boundary condition (b) with $\alpha = 0$. Free energy change (bottom panels in (c),(d)) and its first derivative (top panels in (c),(d)) during compression, for GNRs with (LAGBI, LAGBII) and without (PG) grain boundary for FBC (c) and SBC (d).

Figures 2(a)–2(c) (FBC) and Figs. 2(d)–2(f) (SBC) show snap shots of the deformed GNRs without (a),(d) and with grain boundary (b),(c),(e),(f), beyond the buckling threshold, where $\epsilon = 2.45\%$ and $\alpha = 0$. The strain is calculated using $\epsilon = 2\delta x/l$, where $l = a$ ($l = b$) for $\alpha = 0$ ($\alpha = \pi/2$). From Figs. 2(a)–2(c), we see that the deformed shape for PG is similar to half a sine wave which is much less the case for the LAGBI and LAGBII. The deformations in Figs. 2(d)–2(f) satisfy the condition $m = 1$ in δw, while in the direction of the applied compression for LAGBI and LAGBII, the shape of the deformation is different from a sine wave which is most clearly seen around the grain boundary.

The buckling threshold, i.e., ϵ_b, is measured by finding the sudden increase in the average quadratic out of plane displacement of the GNR atoms ($\langle h^2 \rangle$). The variation of $\langle h^2 \rangle$, averaged over ten simulations for $\alpha = 0$, versus ϵ are shown in Figs. 3(a) and 3(b) for FBC and SBC, respectively. The vertical arrows indicate the transition points to the buckled state. The buckling strains, ϵ_b, are listed in Table I for various situations. We found that graphene with LAGBII grain boundary subjected to FBC vibrates quickly so that the relaxed system (before compression) is buckled and thus the buckling strain is zero. This is due to the larger angle misorientation (32.2°). However, notice that before buckling (FBC), $\langle h^2 \rangle$ for PG fluctuates which is less for LAGBI. Note that a study of the edge reconstruction needs an *ab-initio* approach which is out of the scope of the present study.[16]

Changing α varies ϵ_b significantly. In fact for $\alpha = \pi/2$, the buckling strain for LAGBI is three times larger than for PG indicating a considerable change in the structural deformation of graphene when it is subjected to compressive tension along the grain boundary. As seen from Fig. 3(b), for SBC, the largest (smallest) buckling strain is for LAGBI (LAGBII) and therefore we conclude that graphene with LAGBII is thermodynamically less stable as compared to LAGBI and PG. This is also confirmed by our free energy calculations. Note that a larger angle α grain boundary results in weaker graphene.[17]

TABLE I. Estimated buckling strains for different boundary conditions and different α with and without grain boundary.

α	PG FBC	LAGBI FBC	LAGBII FBC	PG SBC	LAGBI SBC	LAGBII SBC
0	0.6%	0.34%	0.01%	0.7%	1.45%	0.4%
$\pi/2$	1.07%	3.0%	0.2%	—	—	—

The obtained buckling strains are comparable to the one obtained from recent buckling experiments i.e., 0.7%.[18,19] Our theoretical buckling strains are a little smaller than those found in the experiments, which we attribute to the presence of a weak van der Waals interaction between the substrate and graphene in the experiment. Note that strains are more than an order of magnitude smaller than those where fracture occurs in stretching simulations and nanoindentation experiments (they were in the range 10%–30%).[20]

The change in the free energy difference when compressing the GNRs subjected to FBC (SBC) with $\alpha = 0$ is shown in the bottom panel of Fig. 3(c) (Fig. 3(d)). Notice that our non-compressed GNRs (in the beginning of the simulations) are flat honeycomb lattice structures (and during the first equilibration we did not change its size) which are not in a thermomechanical equilibrium state at finite temperature. Therefore, the free energy of this state should be higher than the one of the equilibrium state. The free energy of graphene with LAGBII increases with ϵ, i.e., there are no minima in the free energy curves either for SBC or for FBC. This is a confirmation of our previous argument about the instability of this system when it is suspended.

Notice that the LAGBI system with FBC (SBC) exhibits a minimum, i.e., equilibrium state corresponds to the minimum points in the free energy curve, for larger strains, $\epsilon_m = 0.73\%$ (1.07%) as compared to $\epsilon_m = 0.52\%$ (0.47%) for PG. The reason is that the LAGBI system with a flat surface is much farther from thermodynamical stability than the flat PG. The top panels in Figs. 3(c) and 3(d) show the first derivative of the free energy for FBC and SBC, respectively. Here the transition is continuous because of the finite size of the simulated GNR.

As seen from the bottom panel of Fig. 3(d) at the minimum point in the free energy curve, the rippled state has a lower free energy as compared to the initial non-compressed GNRs, i.e., $\Delta F\ (LAGBI) = -10.5\,\text{eV}$, $\Delta F\ (PG) = -1.5\,\text{eV}$. Therefore, PG (LAGBI) needs less (more) compression steps to reach its equilibrium size.

In summary, we found that deformations of graphene nano-ribbons that are subject to in-plane axial boundary stresses are different when the graphene sheet contains two kinds of grain boundaries with special symmetry with large angle grain boundaries $\theta = 21.8°$ and $\theta = 32.2°$. In the

presence of a grain boundary with $\theta = 21.8^\circ$ the GNR subjected to compression parallel (perpendicular) to the grain boundary has a buckling strain that is largest, i.e., 3% (0.34%) when the lateral edges are free. The grain boundary with large angle $\theta = 32.2^\circ$ results in smallest buckling strains and into an instability when graphene is suspended.

This work was supported by the Flemish Science Foundation (FWO-Vl) and the Belgian Science Policy (IAP).

[1]A. Hashimoto, K. Suenaga, A. Gloter, K. Urita, and S. Iijima, Nature (London) **430**, 870 (2004).
[2]T. R. Albrecht, H. A. Mizes, J. Nogami, S.-I. Park, and C. F. Quate, Appl. Phys. Lett. **52**, 362 (1988).
[3]X. Li, W. Cai, J. An, S. Kim, J. Nah, D. Yang, R. Piner, A. Velamakanni, I. Jung, E. Tutuc *et al.*, Science **324**, 1312 (2009).
[4]O. V. Yazyev and S. G. Louie, Phys. Rev. B **81**, 195420 (2010).
[5]P. Y. Huang, C. S. Ruiz-Vargas, A. M. van der Zande, W. S. Whitney, M. P. Levendorf, J. W. Kevek, S. Garg, J. S. Alden, C. J. Hustedt, Y. Zhu, J. Park, P. L. McEuen, and D. A. Muller, Nature (London) **469**, 389 (2011).
[6]O. V. Yazyev and S. G. Louie, Nature Mater. **9**, 806 (2010).
[7]M. Neek-Amal and F. Peeters, Phys. Rev. B **82**, 085432 (2010).
[8]M. Neek-Amal and F. M. Peeters. J. Phys.: Condens. Matter **23**, 045002 (2011).
[9]M. Neek-Amal and F. M. Peeters, Appl. Phys. Lett. **97**, 153118 (2010).
[10]D. W. Brenner, Phys. Rev. B **42**, 9458 (1990).
[11]J. C. Meyer, A. K. Geim, M. I. Katsnelson, K. S. Novoselov, T. J. Booth, and S. Roth, Nature (London) **446**, 60 (2007).
[12]W. Bao, F. Miao, Z. Chen, H. Zhang, W. Jang, C. Dames, and C. Ning Lau, Nat. Nanotechnol. **4**, 562 (2009).
[13]C. Jarzynski, Phys. Rev. Lett. **78**, 2690 (1997).
[14]M. Neek-Amal, Phys. Rev. Lett. **106**, 209701 (2011).
[15]R. M. Jones, *Buckling of Bars, Plates, and Shells* (Bull Ridge, Virginia, 2006), p. 50–264.
[16]P. Koskinen, S. Malola, and H. Hakkinen, Phys. Rev. Lett **101**, 115502 (2008).
[17]R. Grantab, V. B. Shenoy, and R. S. Ruoff, Science **330**, 946 (2010).
[18]G. Tsoukleri, J. Parthenios, K. Papagelis, R. Jalil, A. C. Ferrari, A. K. Geim, K. S. Novoselov, and C. Galiotis, Small **5**, 2397 (2009).
[19]O. Frank, G. Tsoukleri, J. Parthenios, K. Papagelis, I. Riaz, R. Jalil, K. S. Novoselov, and C. Galiotis, ACS Nano **4**, 3131 (2010).
[20]C. Lee, X. Wei, J. W. Kysar, and J. Hone, Science **321**, 385 (2008).